physica status solidi b
www.pss-b.com

Intrinsic Electrical Conductivity of Silicate Glass Doped with Ruthenium Dioxide: Experimental Evidence

Gulmurza Abdurakhmanov, Avazbek T. Dekhkonov, and Mukhriddin E. Tursunov*

It has been shown experimentally that lead–silicate glass of various compositions itself becomes electrically conductive due to the diffusion of Ru atoms during the firing process. Using energy-dispersive spectroscopy and profiling of the spreading resistance R_S and thermoEMF S on beveled samples, a close correlation between the ruthenium concentration and the distribution of specific resistance and thermoEMF has been shown. Changes of the Ru atoms concentration and the spreading resistance R_S, as well as the thermopower S through the diffusion layer, obey a simple diffusion law (complementary error function), when the diffusion coefficient does not depend on the concentration of diffusing atoms. At a very low concentration of Ru atoms (near the glass-diffusion layer boundary), the thermopower S reaches 5–7 mV K^{-1}, while at the glass–RuO_2 boundary (high concentration of Ru atoms) it is several μV K^{-1}. The calculated diffusion length under normal annealing conditions of thick-film resistors (10 min at 1123 K) exceeds 100 μm, which is many times greater than the average distance (0.5–2 μm) between RuO_2 particles and confirms that the glass matrix becomes uniformly doped and conductive.

1. Introduction

The conduction mechanism of lead–silicate glass doped with RuO_2 or ruthenates (DLSG, well-known as thick-film resistors (TFR)) has been studied for over 50 years.[1–7] DLSGs are typically fabricated by sintering a mixture of submicron powders of a silicate glass and a "conducting phase" (RuO_2 or ruthenates) at a peak temperature of about 1123 K for 10 min (thick-film technology). The main efforts of researchers have been aimed at explaining the mysterious almost parabolic minimum in the temperature dependence of resistance $R(T)$, as well as the exponential change in resistance $R(T) \approx \exp(T_0/T)^{\gamma}$ ($\gamma \approx 0.4$–0.5) at low temperatures down to 0.05 K. Experiments at low temperatures were carried out to confirm the existence of the variable range hopping (Mott mechanism, $\gamma = 1/4$), which was assumed to be the main conductivity mechanism of TFR. Various mechanisms have been proposed to explain $R(T)$: percolation along chains of relict contacting crystalline particles of the conducting phase, tunneling through thin glass layers between these particles, as well as combinations of all these mechanisms with metallic conductivity of the RuO_2 particles. All these proposals are based on the existing of crystalline particles of the conducting phase (RuO_2) distributed almost uniformly in a glass matrix of TFRs and observed in an electron microscope and X-ray diffraction patterns. This point of view exists to this day.[8] However, none of the proposed mechanisms could convincingly describe the experimental temperature dependence of resistance in the temperature range studied, including 1) "metallic" conductivity[9–11] following the resistance minimum and 2) decreasing of the percolation threshold down to 1 vol% or less[12] contrary to the theoretical value (16 vol%) or even its absence. The temperature range of "metallic" conductivity, as well as the minimum of $R(T)$, depends on the glass composition and the content of the dopant. It was also not possible to explain dependence of the electrical conductivity of the TFR on 1) the temperature and duration of sintering of the mixture of powders of glass and ligature; 2) the particle size in the powders; and 3) the glass composition.

Thermopower S of the TFRs has been reported by two groups of researchers: Pike and Seeger[2] reported S has a positive sign and a value of tens of μV K^{-1} (as in metals), Prudenziati et al.[9] showed that $S(T) \approx T^{1/2}$ in the interval $T = 200$–450 K. The authors interpreted the latter fact as evidence of hopping conduction.

It should be noted that the sign of the Seebeck coefficient in doped silicate glass is not related to the sign of the thermopower of the dopant and is positive (holes) in all the cases studied, although in $Bi_2Ru_2O_7$, e.g., it is negative (electrons).[2]

The sharp increase and maxima of resistance and Seebeck coefficient of TFRs at temperatures around 1000 K,[10] which contradict existing ideas, did not attract the attention of researchers.

Only two groups of researchers have attempted to study the distribution of Ru atoms in glass near the glass–RuO_2 layer interface. Abe et al.[13] measured the RuO_2 or Au concentration and resistivity profiles near the glass–RuO_2 layer interface and showed that Ru atoms diffuse deeper into the glass (about 2 μm) than Au atoms. Based on this fact, they concluded that in resistors having a low RuO_2 concentration a reactive layer is formed around the RuO_2 particles, which maintains electrical conductivity of the TFR. However, there is no comparison of

G. Abdurakhmanov, A. T. Dekhkonov, M. E. Tursunov
Physics faculty
National University of Uzbekistan
Olmazor district university street 4, 100174 Tashkent, Tashkent, Uzbekistan
E-mail: dexqonov_@nuu.uz

The ORCID identification number(s) for the author(s) of this article can be found under https://doi.org/10.1002/pssb.202500347.

DOI: 10.1002/pssb.202500347

RuO_2 concentration and resistivity profiles, so it is impossible to assess the role of diffusion in electrical conductivity.

Totokawa et al.[14,15] investigated at nanoscale the piezoresistive mechanisms of TFRs based on RuO_2 particles and both calcium–borosilicate and bismuth–borosilicate glasses. It was confirmed that the diffusion of ruthenium into glass affects the binding state of RuO_2 at the interface of the glass. An intermediate resistive layer was detected around the RuO_2 particles. Unfortunately, the authors did not investigate the diffusion profile of Ru atoms in this intermediate layer, so there is no confirmation of the relationship between the resistivity and the concentration of Ru atoms.

Based on a set of experimental data,[16,17] another conductivity mechanism for TFRs was proposed, suggesting 1) the existence of nanocrystals in the glass itself; 2) structural transitions in nanocrystals at high temperatures; 3) diffusion of atoms of the conducting phase into the glass during sintering and the formation of an impurity zone near the top of the valence band of the glass; and 4) the conductivity of a TFR is the sum of activation conductivity along the impurity band and hopping conductivity across nanocrystals. This mechanism made it possible to qualitatively explain the temperature dependence of the conductivity of TFRs in the temperature range from liquid helium to 1100 K.

However, the assumption about the correlation between the diffusion of atoms of the conducting phase into glass and the conductivity of the glass itself has not been confirmed experimentally.

The article presents experimental evidence of a direct correlation between the concentration of ruthenium atoms, diffusing into silicate glass, with electrical conductivity and the Seebeck coefficient.

2. Experimental Section

2.1. Sample Preparation

To study the correlation between ruthenium diffusion, the electrical conductivity, and the thermopower of doped lead–silicate glass, we prepared a model system of compositions listed in **Table 1**.[18] The batch was melted at 1773 K for 1 h and cast into steel molds, forming prism-like specimens ($20 \times 4 \times 4$ mm). After annealing at 723 K for 3 h, the specimens were polished to optical quality on two long opposing surfaces.

Table 1. Compositions of the glasses researched.

Glass	Components, mass/mol [%]			
	SiO_2	PbO	BaO	MgO
1	33/64.7	67/35.3	–	–
2	27/54.4	67/36.3	4/3.2	2/6.1

The sample was placed with one polished side up in a vessel and filled with an aqueous suspension containing 1 wt% RuO_2. After the suspension had settled for 5 min, the sample was carefully, without turning over, removed from the suspension, and dried for 1 h at a temperature of 423 K. Then the sample with the RuO_2 layer up was placed in an oven and diffusion was carried out for 5 h at 923 K (**Figure 1**a). Such a relatively low diffusion temperature was chosen deliberately to avoid viscous flow and deformation of the sample, while maintaining its geometric shape and surface polishing, which is essential for depth-resolved analysis in the diffusion layer.[14] The diffusion process could be considered as diffusion with constant surface concentration,[19] since according to various authors solubility of RuO_2 in lead–silicate glass is less than 7 mass%.[16] After diffusion, the two side faces of the sample perpendicular to the diffusion layer were polished to optical quality so that the distribution of ruthenium atoms in the diffusion layer could be measured with an energy-dispersive X-ray spectroscopy (EDS).

To convert vertical (across the interface glass–RuO_2 layer) diffusion depth into an extended lateral profile for spatially resolved characterization, a bevel of ≈0.5° was polished on the RuO_2-coated surface (Figure 1b). This approach effectively magnifies the diffusion profile by a factor of about 115, allowing micrometer-scale resolution of chemical gradients over millimeter-scale distances as well as measuring the resistivity and thermopower distribution in the diffusion layer.

2.2. Ru Concentration Measurements

EDS was performed using a JEOL JSM-IT200 scanning electron microscopy (SEM) equipped with an Oxford EDS system (Uzbek-Japan Center for Yong's Innovations). Spectra were acquired both across the RuO_2–glass interface (normal sectioning, x-direction in the Figure 1b) and along the beveled surface (along the l-direction, Figure 1b).[20] To improve signal clarity, spectral noise was filtered using Fourier transform-based smoothing in Wolfram Research Mathematica v. 13.

2.3. Electrical Resistivity Mapping

Distribution of the spreading resistance along the l-direction was measured by single probe, made from tungsten carbide tip of 50 μm radius (Figure 1b), connected to a multimeter Rigol

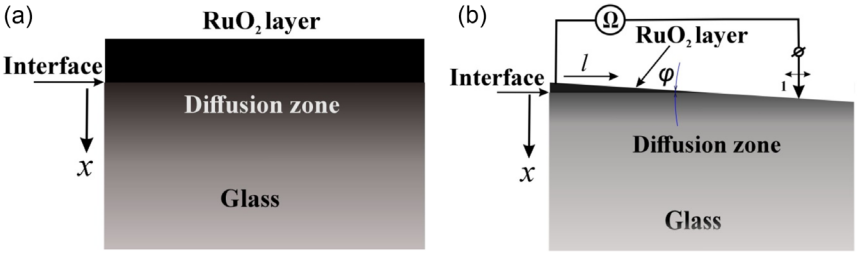

Figure 1. Sample of the glass a) after diffusion and the b) beveled sample with the single mobile probe 1 for spreading resistance and the thermoEMF measurements. Ω—ohmmeter (to measure spreading resistance) or nanovoltmeter (to measure thermoEMF), φ is an angle of bevel.

DM3058E. Thermopower was mapped by the same probe relative to the unpolished end of the RuO_2 layer (left end in Figure 1b) using nanovoltmeter Keithley 2182 A. The tungsten carbide tip was heated by nichrome wire connected to laboratory DC source to generate temperature difference $\Delta T \approx 1.5$ K relative to the glass sample. Temperature difference was measured by the thermal imager Fluke Ti450 Pro (thermal sensitivity 0.025 K at 303 K target temperature) with macro lens 25MAC2.

The resistivity $\rho(x)$ was computed via the classical relation[17]

$$\rho = 2aR_S \tag{1}$$

where R_S is the measured spreading resistance and a is the probe tip radius. This method enabled depth-resolved resistivity profiling with high spatial resolution.

3. Results and Discussion

3.1. EDS Analysis of the Distribution of Components on the Surface of Glasses

EDS analysis showed nonuniform distribution of components on the polished surface of the samples (**Figure 2***a–i*) with a scale of about 30–50 μm. Intensity of the characteristic lines of elements and their content are shown in **Figure 3** and **Table 2**.

Comparison of datum in Table 1 and 2 demonstrates agreement of glass compositions excluding the content of Al and C. Some amount of Al can be dissolved from the alumina crucible in the glass-melting process. And carbon atoms at the sample surface may be adsorbed from the air during storage.

X-ray diffraction patters of the doped glasses 1 and 2 are shown in **Figure 4**a,b.

It is evident from Figure 4 that when doping silicate glasses with RuO_2, most of the dopant remains in the crystalline form, but the reflections of these crystals are shifted relative to the reflections of the free ruthenium dioxide powder, and some reflections have disappeared. This indicates a stressed (deformed) state of these crystals caused by the difference in the thermal expansion coefficients of the glass and the dopant.

3.2. Ruthenium Diffusion Profile

Initial EDS analysis across the interface between the RuO_2 coating and the underlying glass revealed a distinct diffusion profile of ruthenium. The filtered spectrum intensity as a function of depth, $I(x)$, was accurately described by a complementary error function (erfc) of the form

$$I(x) = I_0 \cdot \mathrm{erfc}(\alpha x) \tag{2}$$

which is typical for Fick's law with a constant diffusion coefficient.[21] The filtered distribution of Ru atoms in the glass across the diffusion layer is shown in **Figure 5**.

The wide double maximum at $0.25\ \mathrm{mm} < x < 0.55\ \mathrm{mm}$ corresponds to the RuO_2 layer. Distribution of the Ru atoms in the diffusion layer, described as

$$I(x) = 10 + 320\,\mathrm{erfc}(1.8x) \tag{3}$$

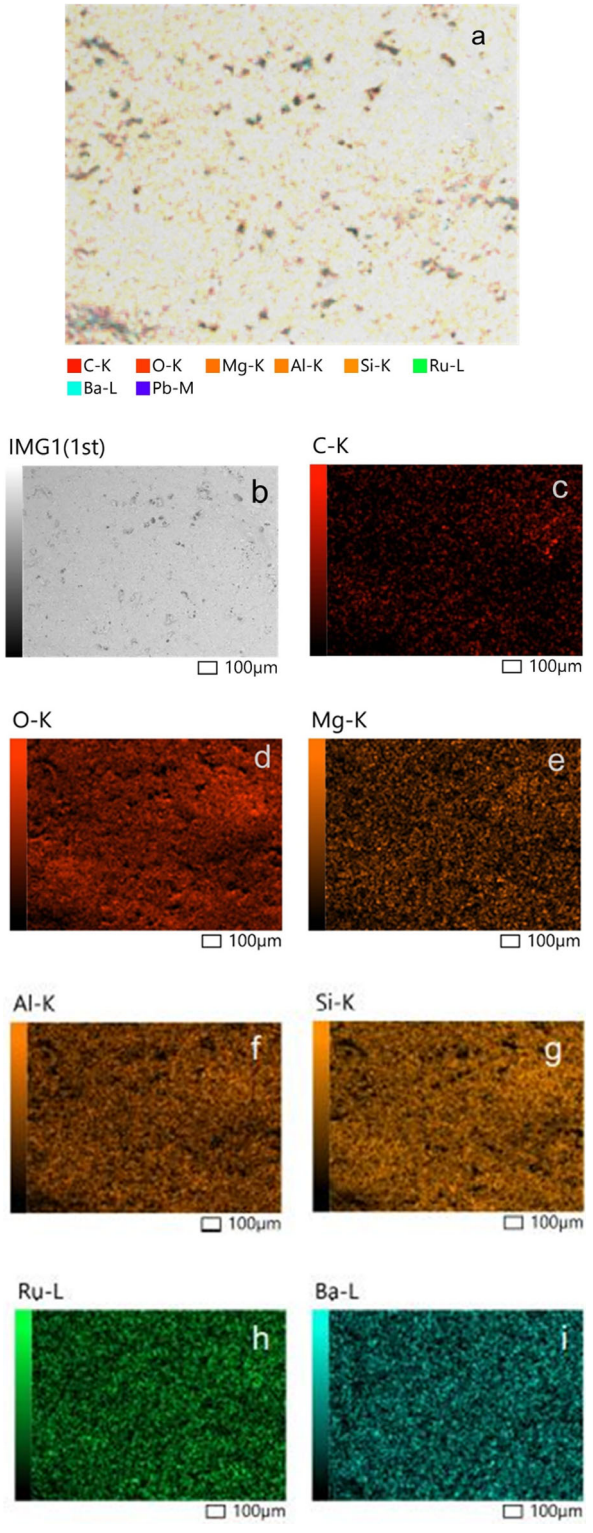

Figure 2. Distribution of components on the polished surface of the doped glass 2 via EDS analyses: a) total view for all elements of the glass 2; b) pattern (a) with scale bar; c) carbon C; d) oxygen O; e) magnesium Mg; f) aluminum Al; g) silicon Si; h) ruthenium Ru; and i) barium Ba. Distribution of the Pb is not shown because of almost uniformity, may be due to large scattering area of its atoms (large number of electrons).

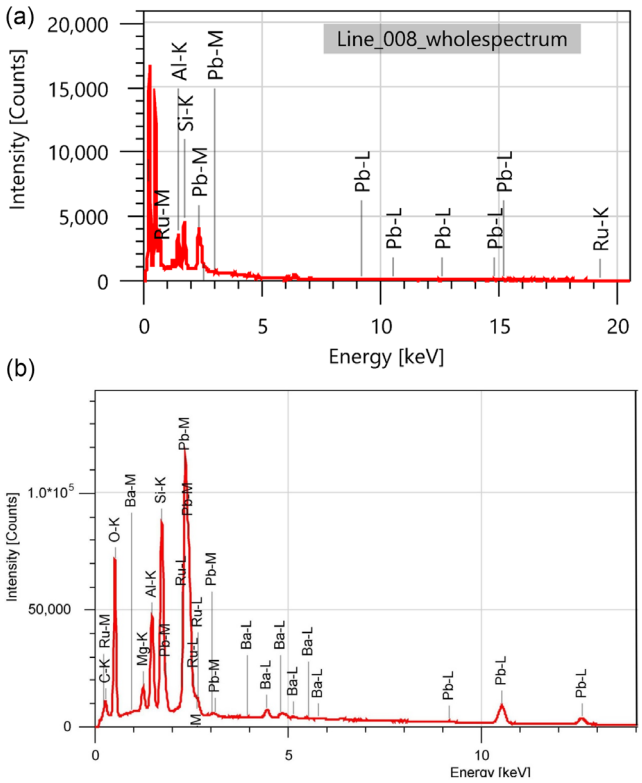

Figure 3. Energy-dispersive spectrum of the polished surface of doped glasses a) 1 and b) 2.

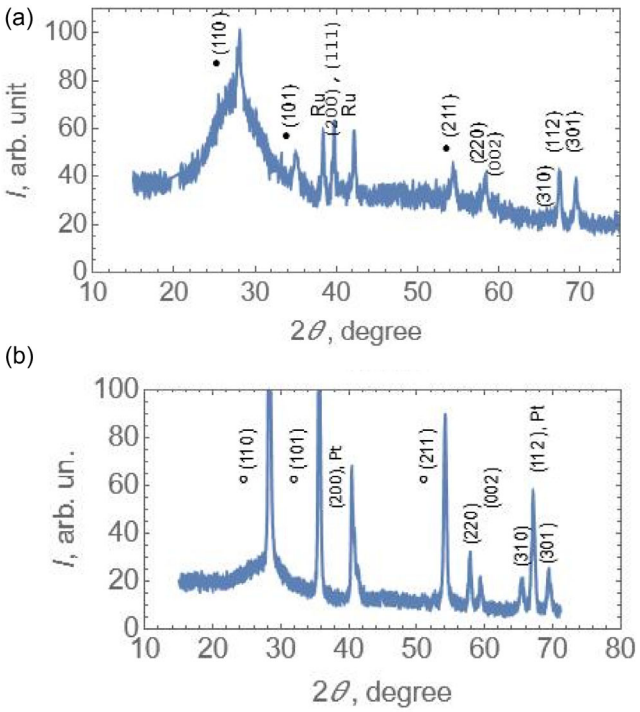

Figure 4. X-ray diffraction patters of the doped glasses a) 1 and b) 2 with crystallographic plane indices of RuO_2. Platinum peaks (200) and (112) are due to the platinum sample holder.

indicates the constant diffusion coefficient (i.e., it does not depend on the concentration of ruthenium atoms at the point in question). One can estimate the diffusion coefficient D(873 K) from the data in Figure 5, keeping in mind that erfc(0) = 1 and erfc(1) = 0.1559. The initial intensity of the EDS spectra $I_0 = I(x = 0.53)$ ≈55 counts; therefore, the intensity $I_0 \cdot \mathrm{erfc}(1) = 55\ 0.1559 = 8.57$ is achieved at the point $x = 1.2 - 0.53 = 0.67$ mm.

Taking into account the fact that the argument of the function erfc(z) is equal to $z = x/2l_d$, we have

$$l_d = x/2 \approx 0.335\text{mm} \tag{4}$$

The dotted line in Figure 5 is the approximation by the function

$$I(x) = 10 + 320 \cdot \mathrm{erfc}(1.8x) \tag{5}$$

then

$$D(873\text{K}) = l_\text{d}^2/\tau = \frac{(3.35\cdot 10^{-4})^2}{18000} \approx 6.2\cdot 10^{-12}\,\frac{m}{s^2} \tag{6}$$

which is in good agreement with the data on diffusion in oxide glasses.[19,22] It is also seen that the diffusion length in the glass (about 0.335 mm) under diffusion conditions (873 K, 5 h) significantly exceeds the diameter of the glass powder particles (0.1–0.2 μm) in TFRs. The standard firing duration of the TFRs at peak temperature is $\tau_s = 10$ min = 600 s, so the diffusion length l_d will be shorter

$$l_\text{d} = 0.335\sqrt{\tau_s/\tau} = 0.06\text{mm} \tag{7}$$

This once again confirms the conclusion of our previous studies[18,23] that during sintering, the entire volume of glass is doped almost uniformly and becomes conductive. In the second experiment, the distributions of the concentration of ruthenium atoms $I(l)$ and the spreading resistance $R_S(l)$ along the beveled sample were measured (Figure 1b). Since the length of the beveled sample is more than 15 mm, and the maximal electronic scanning zone in the SEM is 3 mm, the total EDS was compiled by stitching together five separate spectra. This spectrum has been filtered by Fourier transform as well (**Figure 6**).

Table 2. Content of components on the polished surface of doped glass from EDS analysis.

Glass	Components, mass/atom [%]							
	Si	Pb	Ba	Mg	Ru	Al	O	C
1	12.0/18.8	54.9/11.6	–	–	4.85/2.1	8.65/14.0	19.6/53.5	–
2	8.1/11.5	54.7/10.6	2.6/0.8	1.1/1.8	3.8/1.5	4.2/6.3	21.1/52.9	4.4/14.7

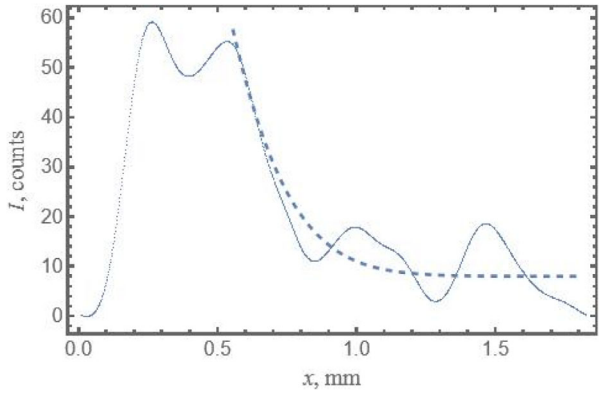

Figure 5. Filtered EDS spectrum of Ru across the diffusion layer.

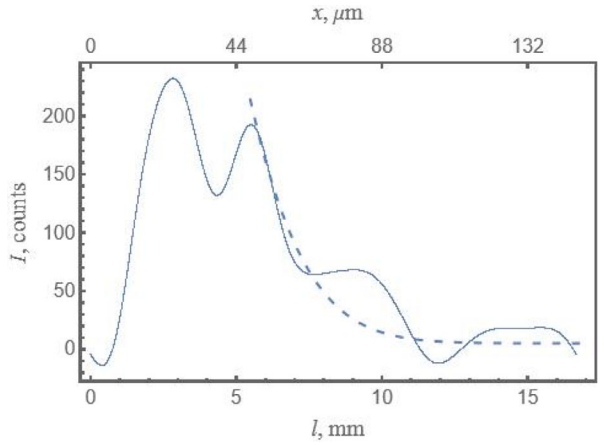

Figure 6. The filtered EDS spectrum of the Ru along the diffusion layer. The dotted line—function $I(x) = 5 + 1600\ \mathrm{erfc}(0.195\ L)$. The meaning of the lower and upper scales, see Figure 1b.

The rescaled distribution of the Ru atoms in Figure 6, described as

$$R_S = 5 + 1600\,\mathrm{erfc}(0.195l) \tag{8}$$

agrees well with the similar distribution in Figure 6. The double maximum at $0.25\ \mathrm{mm} < x < 0.55\ \mathrm{mm}$ corresponds to the unpolished layer of RuO_2 (see above in Figure 5). This confirms the possibility of using a beveled sample to establish a correlation between the concentration of ruthenium atoms and the resistivity distribution in the diffusion layer.

From this fit, the diffusion length was determined as $l_d = 0.335\ \mathrm{mm}$, and the effective diffusion coefficient at 873 K was estimated using the relation $D = l_d^2/t$, yielding

$$D(873\mathrm{K}) \approx 6.2 \cdot 10^{-12}\mathrm{m}^2/\mathrm{s} \tag{9}$$

This value aligns with known cation diffusion rates in silicate matrices and is significantly higher than what would be expected for metallic Ru, confirming that RuO_2—not elemental Ru—is the diffusing species. The magnitude of the diffusion length notably exceeds the average glass particle size (≈0.2 μm) and interparticle spacing in TFRs (≈0.5–2 μm), suggesting uniform doping of the glass phase during firing.

It should be noted that local variations in $I(l)$ or $I(x)$ in Figures 5 and 6 may be caused by nonuniform distribution of components in the studied glass samples (Figure 2), which change the local diffusion coefficient of Ru atoms.

3.3. Correlation with Electrical Conductivity

The beveled sample approach enabled simultaneous mapping of both Ru concentration and local resistivity as functions of lateral position (effectively corresponding to depth x). The EDS signal intensity $I(l)$ along the diffusion layer followed the same erfc behavior (**Figure 7**)

$$I(l) = A + B \cdot \mathrm{erfc}(\beta l) \tag{10}$$

This confirmed the validity of using the beveled geometry for correlating compositional and electrical profiles. Spreading resistance measurements along the bevel revealed a distinct nonlinear resistivity profile, with sharp transitions that closely matched the Ru distribution.

The distribution of ruthenium atoms in the diffusion layer (Figure 6) and the distribution of resistivity in the same layer (Figure 7) are in good agreement with each other. This means that the entire volume of the TFR is involved in the electrical conductivity, and not just the conducting chains (infinite clusters) formed from dopant particles (conducting phase).

Notably, the observed resistivity distribution could be modeled as

$$R_S(l) = \frac{l}{1-kl} \cdot \frac{A}{I(l)} = \frac{l}{1-0.065l} \frac{4.86}{\mathrm{erfc}(0.023l)} \tag{11}$$

where the first factor $1/(1-kl)$ accounts for geometric effects (increasing contact distance and decreasing cross-sectional area with l), and the second $1/\mathrm{erfc}(\alpha l)$ reflects the inverse relation between charge carrier concentration and Ru content.

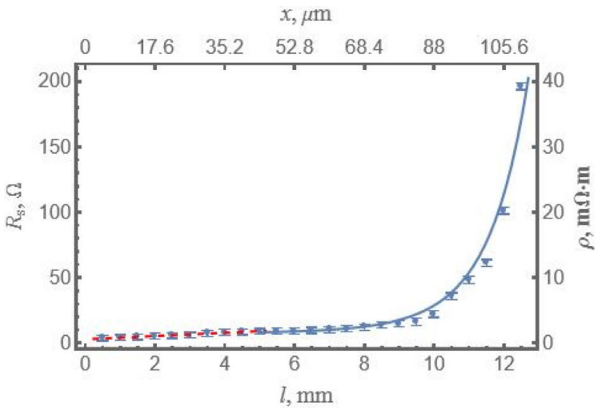

Figure 7. The spread resistance R_S and resistivity ρ distribution along (lower scale) and across (upper scale) the diffusion layer are shown in Figure 1b. Points are experimental data; - - - the function $R_S(l) = 0.0011 + 0.551\ L$; —— the analytical model described by equation $7.5 + 4.86xl/(1 - 0.065l)\mathrm{erfc}[0.023l])$. . See the text above for detailed explanations of these functions.

A is a proportionality coefficient. The linear function $R_S = 0.0011 + 0.551\,L$ in Figure 7 corresponds to the unpolished RuO_2 layer (left end of the sample in Figure 1b). This analytical model yielded excellent agreement with experimental resistance data.

3.4. Conduction Levels (Paths) in Doped Glass

The diffusion zone formed as a result of doping the glass uniformly fills the entire volume of the doped glass sample. Electrical conductivity is carried out through electron exchange between differently charged dopant ions located within this diffusion zone—that is, by the movement of charge carriers within the dopant subzone itself. Therefore, the width of this dopant subzone determines the effective mass m^* of the charge carriers: the narrower the zone, the greater the effective mass m^*.

In doped glass, when the solubility of the dopant or the level of diffusion doping is low (about 7% or less, see above), the average distance between adjacent dopant atoms becomes significantly larger than the spacing between atoms of the glass matrix. As a result, the overlap integral of the wave functions between adjacent dopant atoms is small. This leads to the formation of a narrow dopant subzone and a large effective mass of free charge carriers.

However, as previously mentioned the most widely accepted model for conductivity in doped glass is the percolation theory. According to this theory, the percolation threshold results from the formation of the first (and still the only one when $C \approx C_{cr}$) infinite conductive cluster composed of dopant particles, which spans the entire volume of the sample, from one electrode to the other. Hence, this infinite cluster is not straight, as previously assumed, but rather highly tortuous. Conductivity occurs along the skeleton of this cluster, while its bulk is concentrated in dead ends that do not participate in conduction.[18,23] However, such a representation contradicts experimental data in the case of doped glass.

In fact, the percolation threshold in doped glass often shifts significantly toward lower doping levels in contrast the theoretical predictions, and this shift cannot be explained by experimental error alone. On the other hand, if the single infinite cluster is cut at any point, the sample's resistance should abruptly increase. However, mechanical alteration of the sample's geometry (resistance tuning) shows that only very small changes in resistance can occur when parts of the sample material are carefully removed.

3.5. Implications for Thick-Film Resistors

These results provide direct evidence that the electrical conduction in TFRs is not confined to percolation paths between discrete RuO_2 particles, but instead involves a bulk contribution from the glass matrix itself. The significant diffusion length suggests that during standard firing (850 °C, 10 min), the entire glass phase becomes doped and conductive, supporting previous hypotheses of impurity band conduction mechanisms. Our findings are consistent with nanoscale piezoresistivity studies on Ru-doped glasses and recent spectroscopic evidence for mixed-valence Ru states within the glass.[20] Taken together, the data advocate a shift from percolation-based models to ones that incorporate diffusion-mediated doping and bulk conduction through modified glass networks.

The distribution of the thermoEMF $U(l)$ along the beveled sample of silicate glasses **1** and **2** doped with RuO_2 was measured (Figure 5) and Seebeck coefficient was calculated (**Figure 8**).

The Seebeck coefficient is initially very low (a few μV, the inset) for both samples, but increases sharply with increasing distance from fixed contact achieving 6.5–7.5 Mv K^{-1}. All measured data for $S(l)$ can be approximated with complementary errors function $S(l) = a + b/\mathrm{erfc}[cx]$, with parameters listed in **Table 3**.

As seen from the graph, the thermoelectric response becomes significantly stronger over longer distances in the material. This phenomenon may be associated with diffusion zones formed as a result of the diffusion of Ru atoms throughout the glass matrix. In these zones, the local carrier concentration, electrical conductivity, and potential gradient increase, which contributes to the rise in thermoelectric voltage.

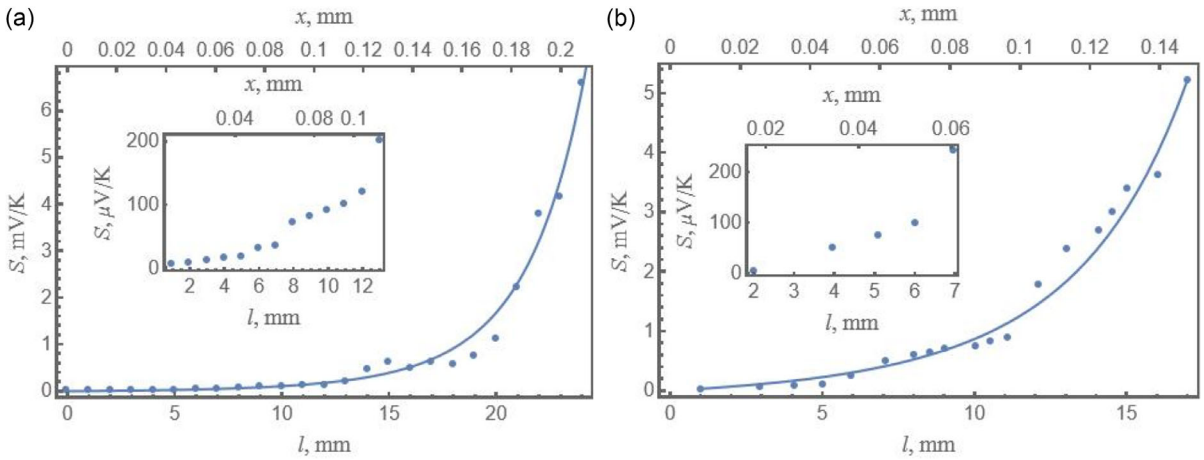

Figure 8. Seebeck coefficient as function of a distance along the beveled sample in Ru-doped silicate glasses a) 1 and b) 2. Insets show enlarged initial parts.

Table 3. Parameters of the approximating function $S(l) = a + b/\mathrm{erfc}[cx]$.

Glass	a	b	c
1	−880	900	0.8333
2	−300	310	0.0793

The Seebeck coefficient for the sample 1 reaches its maximum more quickly compared to sample 2, which may be attributed to differences in the diffusion rate of ruthenium atoms or variations in the local electronic structure. For both samples, the observed increase as erfc(l) suggests that the thermoelectric behavior is influenced not only by the presence of Ru but also by their spatial distribution and interaction with the surrounding glass matrix. Ru atoms diffused into the glass structure, create local electric fields, which affect the motion of electrons or holes and enhance the material's sensitivity to a thermal gradient. The glass with diffused Ru atoms may be considered as p-type semiconductor material, in which Seebeck coefficient is described as[21]

$$S(T) = \frac{k_B}{e}\left[\frac{\mu - E_V}{k_B T} + \alpha_V + 1\right] \tag{12}$$

here μ is the Fermi energy, k_B is Boltzmann's constant, and e is elementary charge. Expression (5) shows that S increases as $\mu - E_V$ due to decreasing concentration of charge carriers (or Ru atoms) in accordance with Figure 8.

In the studied samples, high values of the Seebeck coefficient (even reaching the millivolt per kelvin range) are accompanied by high electrical conductivity (about $10^{-3}\,\Omega\cdot$m) and low thermal conductivity (about 0.5–1.5 $\mathrm{Wm^{-1}\,K^{-1}}$). Therefore, Ru-doped silicate glasses have the potential to serve as high-performance thermoelectric materials.

4. Conclusion

Profiling of the Ru atoms distribution in the beveled samples shows that silicate glass comes uniformly doped by Ru diffusion, resulting in significant bulk conductivity and Seebeck coefficient. The distributions of resistivity and thermopower in the diffusion layer approximated by the erfc function correlate well with the diffusion profile of Ru atoms, indicating that these properties are inherent in the entire volume of the doped glass. The diffusion length of Ru atoms in the lead–silicate glass, determined from diffusion profiles, is $l_d = 0.335$ mm at 873 K for 5 h and the diffusion coefficient is $D(873\,\mathrm{K}) = 6.2\text{–}10^{-12}\,\mathrm{m^2\,s^{-1}}$. Extrapolation of these values of the diffusion length to standard firing conditions of TFRs (10 min at 1123 K) yields $l_D{}^{st} = 0.06$ mm, which significantly exceeds the average distance between dopant particles in TFRs. High values of the Seebeck coefficient (even reaching the millivolt per kelvin range) as well as high electrical conductivity (about $10^{-3}\,\Omega\cdot$m) and low thermal conductivity (about 0.5–1.5 $\mathrm{Wm^{-1}\,K^{-1}}$) suggest good thermoelectric prospect for Ru-doped silicate.

Acknowledgements

This research was supported by grant IL-4821091667 from the Ministry of Higher Education, Science and Innovations of the Republic of Uzbekistan.

Conflict of Interest

The authors declare no conflict of interest.

Data Availability Statement

The data that support the findings of this study are available from the corresponding author upon reasonable request.

Keywords

beveled samples, diffusion coefficients, diffusion profiles, electrical conductivity, resistance and thermopower distributions

Received: July 10, 2025
Revised: August 26, 2025
Published online:

[1] R. W. Vest Conduction Mechanisms in the Thick Film Microcircuits, Final Technical Report **1975**, https://apps.dtic.mil/sti/pdfs/ADA024825.pdf
[2] G. E. Pike, C. H. Seager, *J. Appl. Phys.* **1977**, *48*, 5152.
[3] C. Grimaldi, T. Maeder, P. Ryser, S. Strässler, *Appl. Phys. Lett.* **2003**, *83*, 189.
[4] R. Pflieger, M. Malki, Y. Guari, J. Larionova, A. Grandjean, *Society* **2009**, *92*, 1560.
[5] M. Prudenziati, J. Hormadaly, *Printed Films – Materials Science and Applications in Sensors, Electronics and Photonics*, Woodhead Publishing, Cambridge **2012**.
[6] K. S. R. C. Murthy, *Int. J. Adv. Res.* **2019**, *7*, 238.
[7] A. Kusy, A. W. Stadler, K. Mleczko, D. Zak, S. Pawlowski, P. Szałański1, Z. Zawiślak, G. Grabecki, W. Plesiewicz, T. Dietl, *Ann. Phys.* **1999**, *511*, 589.
[8] M. Wen, X. Guan, H. Li, J. Ou, *Sens. Actuators A: Phys.* **2020**, *301*, 111779.
[9] M. Prudenziati, A. Cattaneo, *Sci. Techn.* **1976**, *3*, 181.
[10] G. Abdurakhmanov, *WJCMP* **2014**, *4*, 166.
[11] R. Nuernberg, N. M. Machado, M. Malki, M. Neyret, *Materials* **2021**, *546*, 152777.
[12] A. Piarristeguy, R. Nuernberg, D. Jouglard, M. Ramonda, R. Arinero, A. Pradel, M. Neyret, *J. Alloys Compd.* **2021**, *876*, 163123.
[13] O. Abe, Y. Taketa, *J. Phys. D: Appl. Phys.* **1991**, *24*, 1163.
[14] M. Totokawa, T. Tani, M. Yoshimura, S. Yamashita, K. Morikawa, Y. Mitsuoka, T. Nonaka, *J. Am. Ceram. Soc.* **2010**, *93*, 481.
[15] M. Totokawa, S. Yamashita, K. Morikawa, Y. Mitsuoka, T. Tani, H. Makino, *Technology.* **2009**, *6*, 195.
[16] K. Adachi, S. Iida, K. Hayashi, *J. Mater. Res.* **1994**, *9*, 1866.
[17] K. Flachbart, V. Pavlík, N. Tomašovičová, C. J. Adkins, M. Somora, J. Leib, G. Eska, *Phys. Stat. Sol.* **1998**, *205*, 399.
[18] G. Abdurakhmanov, *WJCMP* **2011**, *1*, 19.
[19] H. Mehrer, *Diffusion in Solids*, Springer, Berlin, Heidelberg **2007**, ISBN 978-3-540-71486-6.
[20] M. Tursunov, A. Dekhkonov, G. Abdurakhmanov, V. Ksenevich, D. Tashmukhamedova, G. Vokhidova, D. P. Rai, *J. Techn. Phys.* **2025**, *95*, 1375.

[21] Mott formula, https://en.wikipedia.org/wiki/Seebeck_coefficient?ysclid=meprh6wxwe38080264.
[22] S. I. Sviridov, Diffusion and Kinetics of Interphase Interactions in Oxide Glasses, Abstract of the PhD Thesis in Chemical Sciences, *Ph.D. Thesis*, S.-Petersburg, Institute of Chemistry of Silicates **2000**. (In Russian: С. И. Свиридов. Диффузия и кинетика межфазных взаимодействий в оксидных стеклах. Автореф. к. х. н. С.-Петербург, Институт химии силикатов).
[23] G. Abdurakhmanov, *New Insights into Physical Sciences*, Vol. *4*, Book Publishers International, London-Hooghly **2020**.